Design and Evaluation of a Bolted Joint for a Discrete Carbon-Epoxy Rod-Reinforced Hat Section

Donald J. Baker
Vehicle Structures Directorate - ARL
NASA Langley Research Center
Hampton, VA 23681

Carl Q. Rousseau
Bell Helicopter Textron, Inc.
Ft. Worth, TX 76101

Presented at the 11th DoD/NASA/FAA Conference on
Fibrous Composites in Structural Design
Fort Worth, TX
August 26-29, 1996

Design and Evaluation of a Bolted Joint for a Discrete Carbon-Epoxy Rod-Reinforced Hat Section

Donald J. Baker
Vehicle Structures Directorate - ARL
NASA Langley Research Center
Hampton, VA 23681
and
Carl Q. Rousseau
Bell Helicopter Textron, Inc.
Ft. Worth, TX 76101

Abstract

The use of prefabricated pultruded carbon-epoxy rods has reduced the manufacturing complexity and costs of stiffened composite panels while increasing the damage tolerance of the panels. However, repairability of these highly efficient discrete stiffeners has been a concern. Design, analysis, and test results are presented in this paper for a bolted-joint repair for the pultruded rod concept that is capable of efficiently transferring axial loads in a hat-section stiffener on the upper skin segment of a heavily loaded aircraft wing component. A tension and a compression joint design were evaluated. The tension joint design achieved approximately 1.0% strain in the carbon-epoxy rod-reinforced hat-section and failed in a metal fitting at 166% of the design ultimate load. The compression joint design failed in the carbon-epoxy rod-reinforced hat-section test specimen area at approximately 0.7% strain and at 110% of the design ultimate load. This strain level of 0.7% in compression is similar to the failure strain observed in previously reported carbon-epoxy rod-reinforced hat-section column tests.

Introduction

A primary objective in the development of affordable composite primary structures is to lower recurring manufacturing costs. One approach to lower manufacturing costs is to substitute prefabricated pultruded rods of unidirectional carbon-epoxy material for unidirectional tape. The prefabricated rods have higher stiffness and strength than an equivalent section of tape because the straightness of the fibers is maintained during the manufacturing of the rods. A typical application for the pultruded carbon-epoxy rods is shown in figure 1. In this structural concept the carbon-epoxy rods are embedded in a syntactic film adhesive and laminated with all-bias-ply carbon-epoxy tape. The rods are utilized in a packed "rodpack" form to fabricate the high-stiffness region in the cap and at the base of the hat-section stiffener that is incorporated into a composite wing panel. The pioneering development in this area, outlined in References 1-4, has been accomplished by Bell Helicopter Textron Inc., NASA, and the U.S. Air Force. While the use of prefabricated rods in structural panels does reduce recurring manufacturing cost, it has a perceived limitation that it may be structurally difficult and inefficient to transfer load into and out

of the rod members at a joint or to effect a repair of a damaged component. To address this technical issue, a program was initiated to develop a bolted-joint concept suitable for efficient transfer of an axial load into or out of a rod-reinforced hat-stiffened panel section.

The primary objective of the current investigation is to develop a design of a bolted joint to transfer load into and out of a rod-reinforced hat-section wing stringer such as the stringer shown in figure 1 developed in the U. S. Air Force Design and Manufacture of Low Cost Composites-Bonded Wing (DMLCC-BW) Program (References 1 and 2). The objective of the DMLCC-BW program was to achieve a 50% reduction in manufacturing cost of a composite V-22 wing and a 25% reduction in support costs. The V-22 tip-to-tip wing design studied in References 1 and 2 does not require the load to be transferred out of the stringers at a discrete point. However, repair of a severed stringer or attachment of a wing box test element to a vertical strongback would require this capability. The overall compressive design allowable strain used in the DMLCC-BW program is 0.45%, which takes into account environmental, statistical, and damage tolerance knockdown factors.

The present paper presents the analytical and experimental results of a study of a mechanically fastened joint for the carbon-rod-reinforced hat-section stringer (figure 1) of the V-22 wing upper surface and a metal fitting. The fitting was designed as a metallic hat-to-lug adapter to facilitate subelement specimen testing, but the fitting configuration and extensional stiffness (EA) are amenable to a two-sided-access carbon-epoxy composite repair design.

Specimen Design

The approach used in validating a bolted joint concept is to: (1) perform a preliminary design using conventional techniques to identify the most significant design variables, such as the number of fastener rows, the size and number of fasteners, and the need for reinforcement such as doublers; (2) perform a parametric study that includes a detailed finite element model of a rod-reinforced hat-section stringer segment, a composite doubler, and a bolted metallic fitting; and (3) fabricate tension and compression specimens, instrument the specimens and test them to failure.

Preliminary Design

The primary assumptions and ground rules of the DMLCC-BW program that are applicable to the current program are included as part of this investigation and are as follows: (1) no bolt holes will be located in the rodpacks; (2) all-bias-ply-skins will be used for shear load transfer and; (3) all bolts will pass through the webs and flanges. A number of additional ground-rules imposed as part of this program are: (1) the hat section shall transfer its load into a coaxial fitting (conceptually similar to a repair); (2) the maximum allowable length of the splice will be 13 inches, which is half the length of the shortest bay in the V-22 wing; (3) the centroids of the hat-section stringer, fastener pattern, and fitting shall be located vertically within 10 percent of one-another to minimize eccentricies and associated local bending stress; (4) although the fitting used in this program is metallic (in order to more easily interface with the test machine), the average extensional stiffness (EA) of the fitting shall be in the feasible range for composite materials (i.e., aluminum rather than steel); and (5) the stringer will remain constant in cross-section (i.e., not scarfed), but that the metallic fitting would be tapered to minimize peak loads in the first row and the last row of fasteners.

The desired failure mode is a net-section tension or compression failure in the stringer at the last (i.e., innermost) row of fasteners. Ideally the design strain-to-failure should be 1.5%, which is the maximum tensile strain of an individual rod. Upon careful consideration however, it was evident that tensile failure would probably be limited to around 0.9% strain by the Filled-Hole-Tension strength of the all-bias-ply flange and web laminates. Single hat-section stringer compression testing (reference 4) and simple beam-on-elastic-foundation modeling suggests that 0.70% strain would be the limiting value in compression. Given the DMLCC-BW design allowable of 0.45% strain, a room-temperature mean-test design requirement would be 0.60% strain, after increasing the 0.45% strain for environmental and statistical effects. Thus, 0.60% strain equates to a test design ultimate load (DUL) of 141 kips, for the DMLCC-BW upper-cover stringer design.

The first step in defining the specimen was to check the shear transfer capability of the hat-section webs and flanges and the relative load capacities of the cap and the skin rodpacks. Based on relative rod areas, the cap and skin rodpacks should share the load in a 1:2.43 ratio. The shear transfer capability of the hat-section stringer is governed by the cap-to-web transition since the lower rodpack has a much greater area across which to transfer by shear its portion of the load (i.e., interleave bias plies, skin, and webs for the skin rodpack) compared to only the 10 interleaved bias plies in the cap. Based on the shear strength of a [±45°] carbon-epoxy laminate, the hat-section stringer should ideally be able to transfer 32 kips/inch in the webs and flanges.

In the preliminary stages of this configuration assessment, a maximum strain goal of 1.2% in the hat-section stringer was used, rather than the test DUL of 141 kips, in order to demonstrate the ideal repair capability. Given that the baseline stringer extensional stiffness EA = 23.44 x10^6 psi-in^2 (in tension), then the maximum load P_{max} = 281.3 kips, and the minimum joint length would be 8.8 inches. An assumed fastener pattern of ten effective rows on a one-inch pitch led to the selection of preliminary fastener quantities and sizes of four 3/16 inch blind bolts per inch in each web, and one 1/4 inch bolt per inch in each flange. This preliminary check also confirmed that an eight-ply doubler would be required in order to lower the bearing stresses and to solve an edge-distance problem on the flange.

Using these initial assumptions, a preliminary joint sizing was made using a simple one-dimensional (1-D) joint equilibrium model. This model enforces axial equilibrium and displacement compatibility for a single lap joint. This preliminary effort consisted of estimating fastener loads using the 1-D model, then checking the composite web, composite flange, and the metal fitting for bearing strength; the fasteners for shear strength; the web, flange, and fitting for net-section tension strength; and the rodpack-to-bias-plies laminate transitions for shear strength. Given the ground-rule that the hat-section stringer, fastener pattern, and fitting eccentricities should be minimized, the thickness of various segments at each of the ten axial stations (and associated taper ratios) were then sized. Finally, the tension lugs that interface with the test machine were designed using an existing lug-pin analysis program. At this point, it was then possible to refine the design by determining more accurate bolt loads using a detailed finite element model.

Parametric Finite Element Analysis

A parametric finite element analysis was performed using ANYSYS 5.0a SOLID45, SOLID64, and BEAM4 elements and a linear solver. An existing ANSYS 4.4a global model of the upper-skin stringer segment (Reference 4) was used as a starting point for the model. An

input file for ANSYS was created which incorporated variable expressions for parameters such as fitting taper ratios, thicknesses and bolt pattern details. Three-dimensional views of the initial stringer-doubler-metal-fitting configuration are shown in figures 2 and 3. The transition and load introduction portions of the fittings (both tension and compression joint designs) were modeled using rigid bar elements, and are not shown in figures 2 and 3. Section cuts through the mesh at the noted axial stations are shown in figures 4 through 6 and the BEAM4 mesh of the initial bolt pattern is shown figure 7. The pertinent variables used in this parametric study are listed in Table 1 and are illustrated in figure 8. Thirteen tensile loading cases were analyzed in order to optimize the fitting design. One compressive loading case was analyzed for the tensile fitting design (conservatively assuming tensile EA properties), verifying that the bolt loads were similar to the tensile loading case. No specimen end load was allowed in the compression specimen, all loads were carried by the bolts in the joint. The final values for the design variables used in the parametric study are shown in Table 2. Due to the size of the model and disk space limitations on the workstation where ANYSYS was located, a buckling analysis of the compression specimen was not performed. However, based on the slenderness ratio of the hat-section stringer by itself and recent beam-on-elastic foundation analysis, it is not anticipated that any form of center support will be required in order to prevent global buckling of the compression specimen. No unusual conditions were found in the detailed analysis and the parametric study. Both initial and final values of the parametric variables are shown in Table 2.

Final Design

An important assumption made early in the program that the interaction between bearing and by-pass stresses typically accounted for in conventional bolted composite design was not present for the all-bias-ply laminates with the bolts. Rather, the full bearing capability of the all-bias-ply laminate was present regardless of the by-pass strain. Thus, the specimen ultimate load (SUL) is 172.3 kips (0.735% strain in hat-section stringer) based on the bias-ply bearing ultimate strength at bolt number 210 shown in figure 8. If a conventional bearing/by-pass allowable curve is used (room-temperature dry with mean ultimate strength), an allowable strain of 0.39% is determined, which corresponds to approximately 53% of SUL.

A load of 114.9 kips produces a load in bolt number 210 that initiates fitting yielding and is thus identified as the specimen limit load (SLL). This load generates 0.49% strain at the centerline of the hat-section stringer. Unlike an airframe stress analysis, localized bearing yielding in the fitting was allowed between design limit and design ultimate loads. Determining design limit load (DLL) as 2/3 of DUL (141 kips) yields 94 kips (0.40% strain). Thus, the fitting design promises some margin above the DMLCC-BW DLL and DUL, but only if the conventional bearing/by-pass interaction allowable method is ignored.

At a specimen ultimate load of 172.3 kips, the composite material is marginal in shear strength between the web and the cap rodpack near the outboard end of the fastener pattern, and in bearing strength at the inboard end of the pattern. The failure load of the fitting is 224.9 kips and the failure mode is net-section tension (thought to be well beyond the strength of the composite material).

Photographs of the final assembled tension and compression fittings are shown in figures 9 and 10, respectively. The addition of cutouts in the inboard end of the fittings and changes in the fastener pattern are two design changes that are apparent in comparing figures 2 and 3 to figures 9 and 10. Other changes, as noted in Table 2, have been made to thicknesses, taper ratios, and

fastener diameters. The test specimens shown in the figures are symmetrical about the centerline except for the thicker lug on one end of the tension specimen which was required for adapting the specimens to fit existing test machine clevises. The hat-section specimen used in the tension test was 36.5 inches long by 7.5 inches wide with a joining area of 12.75 inches. The hat-section specimen used in the compression test was 25.38 inches long by 7.5 inches wide with a joining area of 11.25 inches. The fittings are made from 7050-T7452 aluminum. As shown in Table 2, the fitting area at the inboard end of the specimens has been decreased as much as possible in order to minimize the loads in the fasteners numbered 210 and 418 shown in figure 8.

Fabrication and Assembly

Four test specimens denoted T-1 and T-2 for the tension joints and C-1 and C-2 for the compression joints were fabricated for testing. The stringer sections for all specimens were cut from one 52-inch-long three-stringer panel, fabricated by Bell Helicopter Textron Inc. (BHTI) Research Laboratory and Manufacturing R&D personnel using an existing inside mold line (IML) tool (References 1 and 2). The bonded doublers shown in Figure 2 were fabricated separately on a temporary tool formed from the Invar IML tool, tapers were machined on the ends, and then the doublers were bonded to the specimens with AF163 adhesive at 250°F in an autoclave. The 7050 aluminum alloy fittings were machined from thick plate stock, with pilot holes in all fastener locations on the upper fittings. The first two fittings (one each for the tension and compression specimens) were masked, located with three to five flange bolts, and liquid shim was applied to specimens T-1 and C-1 to fill any gap between the doubler and the aluminum fittings. After the unmasking and relocating operations, the remaining fastener holes were drilled and fasteners were installed. The flange fasteners were protruding head bolt-nut-washer combinations. The web fasteners were a combination of blind swaged bolts and conventional metallic rivets (installed with aluminum shim backing plates to simulate blind swaged bolts). This assembly process was repeated for specimens T-2 and C-2, following the testing of specimens T-1 and C-1 to failure. New tension fittings were fabricated for specimen T-2, while the original compression fittings from specimen C-1 were reused for specimen C-2.

Test Procedure

All tests were performed at room temperature in the as-fabricated condition. No environmental conditioning was performed on any specimen. The tension specimens were installed in a 1200-kip test machine as shown in figure 11. The compression specimens were installed in a 300-kip test machine as shown in figure 12. All loads were applied at a rate of 30,000 pounds per minute. The test specimens were loaded to the SLL and unloaded, then loaded to SUL (or failure) and unloaded, then loaded to failure. The loading schedule used for the structural testing of the joints is shown in Table 3.

Each test specimen was instrumented with approximately 40 strain gages. Most gage locations are shown in figures 13 and 14. The gages are placed back-to-back at the locations shown. One linear variable displacement transducer (LVDT) was used to measure the change in specimen length between the pins on the tension specimen. Five LVDT's were used on the compression specimen to measure specimen shortening and out-of-plane deflection at the center

of the specimen. The load, strain, and deflection measurements were recorded with a computer-controlled data acquisition system for each test.

Results and Discussion

A summary to the experimental results is given in Table 4. This table gives the failure loads and the average strains in the hat-section stringer net sections. The average strain is the average of the results from the six strain gages at the center of the specimen.

Tension Test Specimens

No anomalies were found in any of the strain gage results when the tension specimens were loaded to the SLL and SUL. A plot of the results from a strain gage located between bolts 209 and 210 (see figure 8) is shown in figure 15. The nonlinear hysteresis indicated in the figure can be expected from the loading and unloading of the fasteners, but some yielding of the fitting is evident after loading to the SUL. The strain in the specimen returns to zero after the load is removed and follows approximately the same loading path for each load cycle. The results from a gage located between bolts 209 and 210 in the opposite flange are identical to the results shown in figure 15. A plot of the results from the six strain gages at the center of the specimen is shown in figure 16 for specimens T-1 and T-2. The computed strain is also shown in figure 16. The experimental strain compares well with the computed strain. There is also a good comparison between the two tension specimens. The EA for each specimen was determined by computing the average of the slopes of each of the six strain gage result curves, and are shown in Table 4. These experimental EA values are within -1.5 percent and 2.5 percent of the computed EA value of 23.44×10^6 psi-in^2. The failure load was 232.2 kips for specimen T-1 and 237.2 kips for specimen T-2. Both specimens failed in net-section tension of the fittings (within 3.2% and 5.5%, respectively, of the predicted fitting strength). The specimens failed at approximately 135% of the expected SUL and 166% of the DMLCC-BW DUL. Strain gage results at three locations on the centerline of the aluminum fitting are shown in figure 17. The three locations are in the joint area of the rod-reinforced hat-section specimen. The strain in the fitting at failure varies from 0.35% near the fitting runout to 0.75% between the last bolt and the end of the hat-section specimen. The material in the fitting starts to yield at a strain of approximately 0.4 percent. The specimen elongation between the loading pins is shown in figure 18 as a function of the load. Specimen T-1 exhibited approximately 0.05 inch more elongation at failure than specimen T-2.

Failed tension specimens are shown in figure 19. Specimen T-1 failed through bolts 101, 301, and 401 at the end of the specimen with the thin lug as shown in figure 19a. Specimen T-2 failed through bolts 201, 301, 401, and between 101 and 102 at the end of the specimen with the thin lug as shown in figure 19b. Bolt 101 then pulled through the composite hat-section flange cutting a slot in the flange. Failure occurred between the strain gages denoted by the diamond and the circle on the sketch in figure 17. No visual damage at any of the holes in the composite hat-section was noted on disassembly of specimen T-1, however, damage was observed at two 0.250-inch-diameter holes in the flange of specimen T-2.

Compression Test Specimens

A plot of the results from the six strain gages at the center of compression specimen C-1 is shown in figure 20 for a load cycle to the SLL of 115 kips. The divergence of the back-to-back

gages shown in figure 20 indicates that bending is present at the center of the specimen. The test results for columns with six gages at the specimen centerline shown in reference 4 indicate that all gages except the gage on the cap of the hat have similar responses. The test and analysis results given in reference 4 indicate that the strain in the cap is less than the strain in the remainder of the cross-section. The strain in the cap (circle and dashed line) shown in figure 20 is greater than the strain in the skin (circle and solid line). A plot of the results from the six strain gages at the center of specimens C-1 and C-2 is shown up to failure in figure 21. The results from both specimens indicate that bending occurs in the specimens which could be the result of the differences between the centroids of the hat-section stringer, bolt pattern, and aluminum fitting. Bending has the effect of increasing the strain in the cap of the hat, counteracting its natural tendency to unload in compression. Plots of the out-of-plane displacements at the centerlines of specimens C-1 and C-2 are shown in figure 22 as a function of load. The center of the cap of the hat has the least out-of-plane deflection while the flange free edges have the maximum deflection of approximately 0.075 inches.

The average EA measured for each specimen is shown in Table 4. Due to both the lower compression modulus of the carbon-epoxy material (calculated EA $=21.1 \times 10^6$ psi-in^2 versus 23.44×10^6 psi-in^2 in tension) and the bending and local buckling induced in specimens C-1 and C-2, the compressive EA values are approximately 80% of those measured in tension and 92% of those predicted in compression. The failure loads are 155.1 kips for specimen C-1 and 154.8 kips for specimen C-2. The specimens failed at approximately 122% of the SUL and 110% of the DMLCC-BW DUL. The average strain at the location denoted by the filled circle (figure 21) is approximately 0. 7% which is near the average failure strain value for the column specimens tested in reference 4. Strain gage results at three locations on the centerline of the aluminum fitting are shown in figure 23. The three locations are in the joint area of the rod-reinforced hat-section specimen. The results shown in figure 23 indicate that bending occurs at the location denoted by the filled square on the sketch and reduces to very little bending at the end denoted by the filled circle on the sketch. The specimen shortening is shown in figure 24 as a function of load for both compression specimens. Good correlation exists between the specimens.

The failed compression specimens are shown in figure 25. Although the strains at the specimen centerlines were similar (see figure 21), the specimens failure modes were different. Specimen C-1 (see figure 25a) failed in the cap of the hat by pulling apart, like a tension failure. The rods in the skin reinforcement are also pulled apart, while the skin is buckled and delaminated from the doublers and flanges of the hat section. The cap of specimen C-2 (see figure 25b) failed in compression and the layer ends pushed between adjacent plies as shown in figure 26. The skin has buckled, failed, and delaminated from the doubler and the flange. The rods in the skin reinforcement have failed and pushed between adjacent plies as shown in figure 26. No visual damage at any of the holes in the composite hat-section on either specimen were detected on disassembly.

Concluding Remarks

A bolted joint concept suitable for transferring an internal load into and out of a rod-reinforced hat-section has been developed. The design concept is a coaxial single-stringer-metallic fitting for transferring the load into and out of the rod-reinforced hat-section, and is representative of a two-sided repair. Hand calculations were used for preliminary sizing of the

joint. The bolt pattern and fitting geometry were optimized using the results of a finite-element-based parametric study. An aggressive "no-interaction" assumption was made for bearing/by-pass allowables in the all-bias-ply flange and web attachment regions of the stringer.

The tension joint design achieved approximately 1.0% strain in the carbon-epoxy rod-reinforced hat-section stringer and failed in the metal fitting at 135% of the expected specimen ultimate load. The tension joint failed at 166% of the design ultimate load. The compression specimen failed in the carbon-epoxy rod-reinforced hat-section test area at approximately 0.7% strain and 122% of the expected specimen ultimate load, and 110% of the design ultimate load. This strain level of 0.7% in compression is similar to the failure strain observed in earlier carbon-epoxy rod-reinforced hat-section column tests.

Neither the tension nor the compression specimens failed in the bolted joint region, demonstrating that the joint is not the weak link in the design for static loading conditions, and the results suggest a suitable design margin of safety.

References

1. Nunn, K. E. and Dompka, R. V., "DMLCC-BW Phase I Interim Report for Period October, 1991 - October, 1992," WL-TR-92-8009, November 1992.

2. Nunn, K. E. and Dompka, R. V., "DMLCC-BW Phase II Interim Report for Period October, 1992 - October, 1993," WL-TR-92-8007, October 1994.

3. Baker, D. J., Nunn, K. E., Rogers, C. W., Dompka, R. V., and Holzwarth, R. C., "Design, Development and Test of a Low-Cost, Pultruded-Rod Stiffened Wing Concept and Its Application to a Civil Tiltrotor," Proceedings of the 10th DOD/NASA/FAA Conference on Fibrous Composites in Structural Design, NAWCADWAR-94096-60, April 1994.

4. Rousseau, C. Q., Baker, D. J., and Chan, W. S., "Analysis and Testing of a Rod-Reinforced Hat-Section Stringer," 36th AIAA/ASME/ASCE/AHS/ASC Structures, Structural Dynamics, and Materials Conference, New Orleans, LA, April 10-12, 1995; AIAA Paper No. 95-1509.

Table 1. Parametric study variables and nomenclature.

Variable/ Nomenclature	Description, units
m	Slope of flange taper, inch
mc	Slope of cap taper, inch
tcf	Final, e.g., inboard cap thickness, inch
xtpr	x-coordinate at start of widthwise fitting taper, inch
xn	x-coordinate at start of notch, inch
Nr()	Number of bolts in row number()
Dr()	Diameter of bolts in row number(), inch
r	Row number, as shown in figure 8
xyz	Three digit bolt id - x = row, yz = position along row

Table 2. Initial and final values of parametric variables.

Variable/ Nomenclature	Initial Value	Final Value
m	-0.0185	-0.0038
mc	-0.0433	-0.0025
tcf	0.100	0.120
xtpr	9.25	9.25
xn	(no notches)	10.75
Nr(1)	2	8
Dr(1)	0.313	0.250
Nr(2)	4	10
Dr(2)	0.313	0.250
Nr(3)	7	2
Dr(3)	0.250	0.250
Nr(4)	12	18
Dr(4)	0.190	0.188
Nr(5)	8	3
Dr(5)	0.250	0.250
Nr(6)	12	17
Dr(6)	0.190	0.188
Nr(7)	8	0
Dr(7)	0.250	0

Table 3. Loading schedule for tension and compression joint specimens.

Specimen Design Condition	Applied Load, kips	Test Section Strain (P/AE), percent
Limit Load	114.9	0.49
Ultimate Load	172.3	0.735
Maximum Load [a]	224.9	0.96

[a] Based on the net section ultimate strength of the fitting.

Table 4. - Summary of test results.

Specimen Number	Failure Load, kips	Average Strain,[a] percent	Measured EA, Msi-in^2
T-1	232.2	1.02	23.08
T-2	237.2	0.99	24.05
C-1	154.8	0.90	18.81
C-2	155.1	0.86	19.84

[a] Average of six strain gages at specimen centerline.

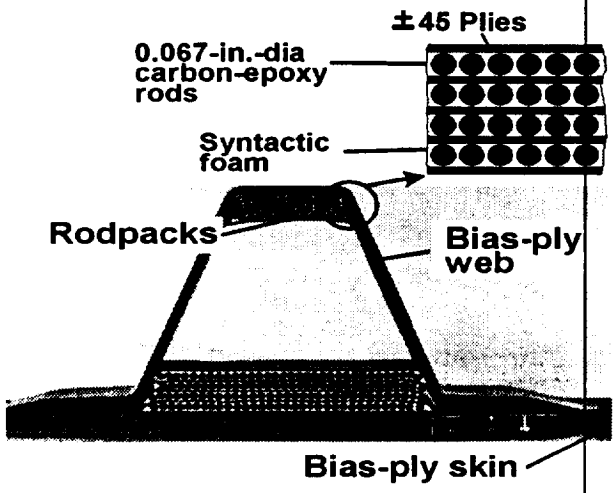

Figure 1. - Rod-reinforced hat-section.

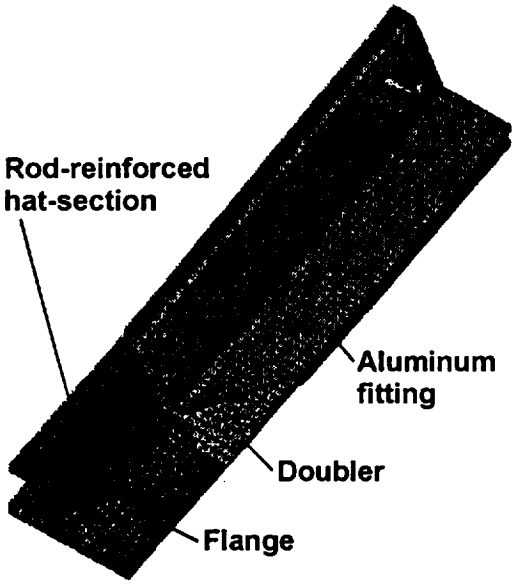

Figure 2. - Upper view of initial stringer-doubler-fitting configuration.

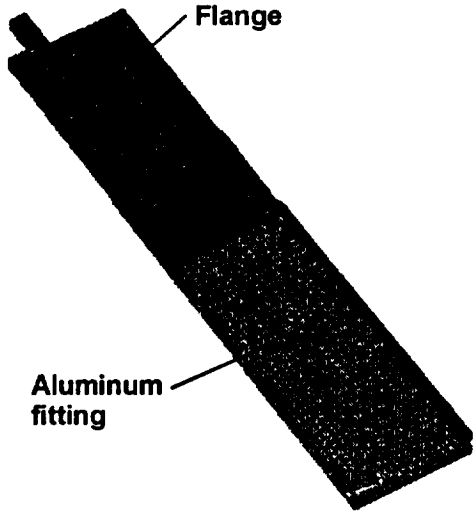

Figure 3. - Lower view of initial stringer-doubler-fitting configuration.

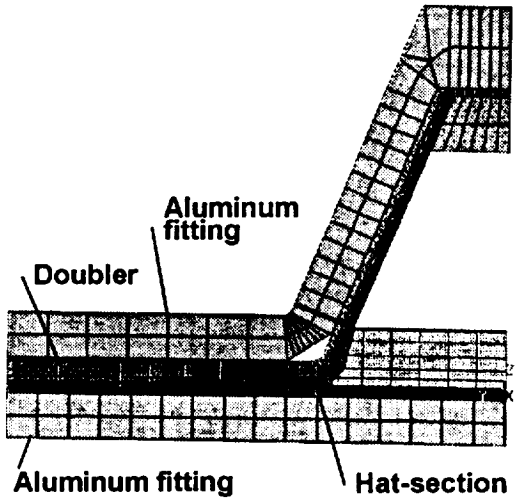

Figure 4. - Cross-section of initial stringer-doubler-fitting at outboard end of stringer.

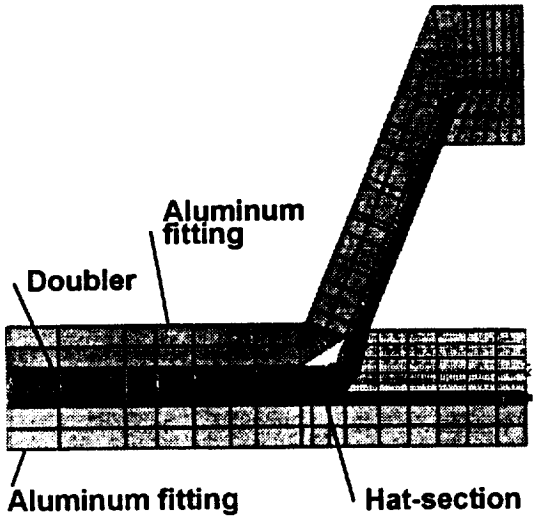

Figure 5. - Cross-section of initial stringer-doubler-fitting at outboard bolt row.

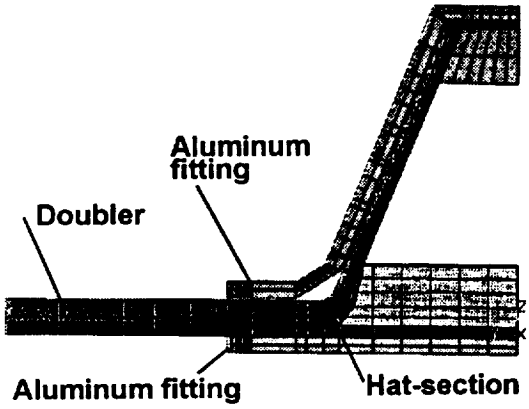

Figure 6. - Cross-section of initial stringer-doubler-fitting at inboard bolt row.

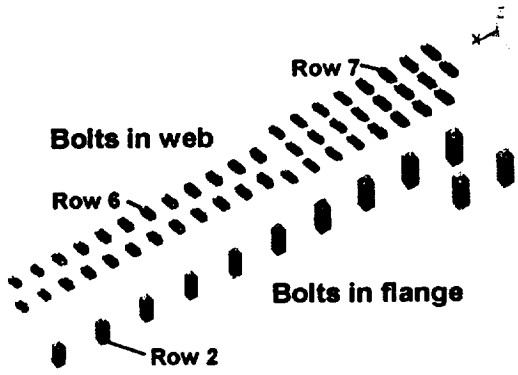

Figure 7. - BEAM4 mesh of initial bolt pattern.

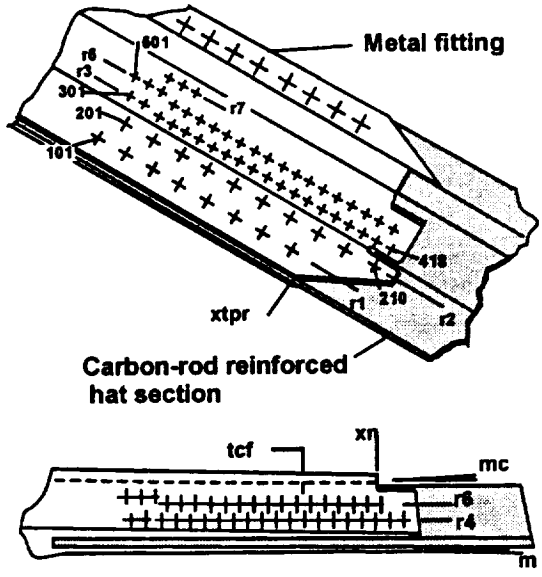

Figure 8. - Variables used in the parametric study.

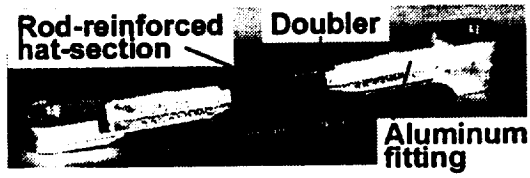

Figure 9. - Assembled tension test specimen.

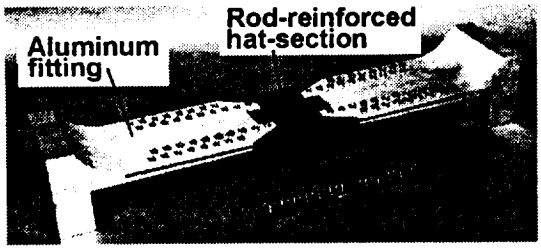

Figure 10. - Assembled compression test specimen.

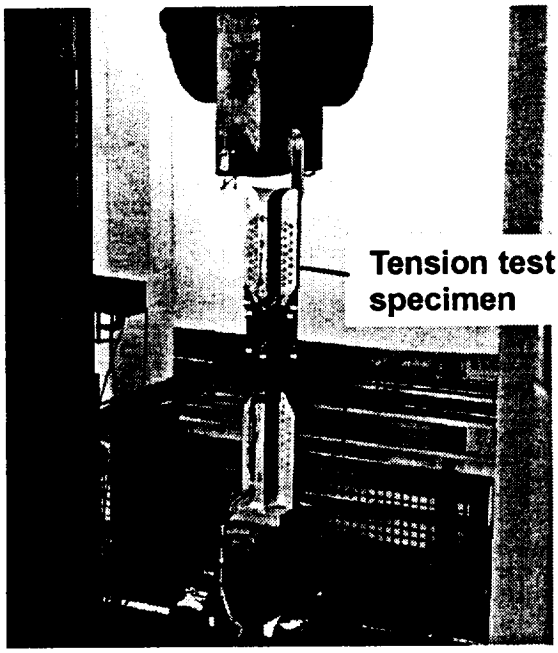

Figure 11. - Tension test specimen installed in 1200-kip test machine.

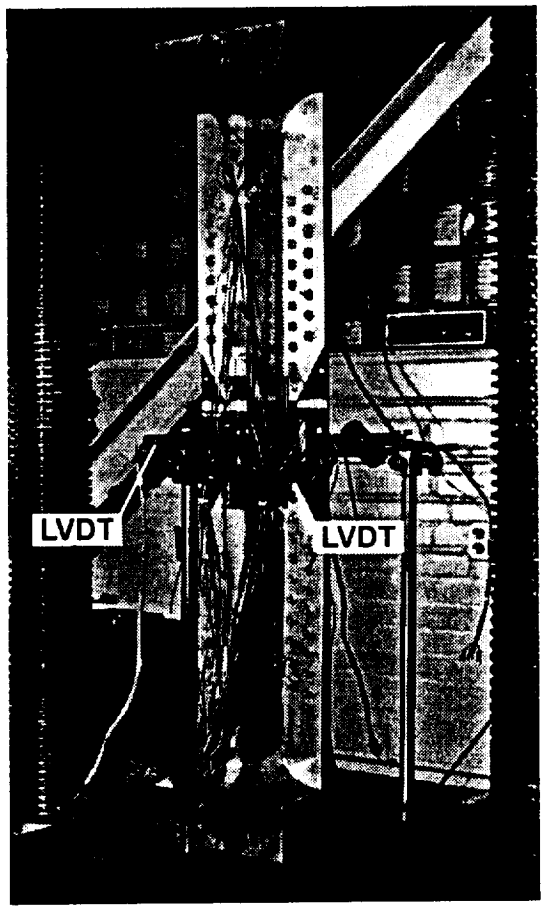

Figure 12. - Compression test specimen installed in 300-kip test machine.

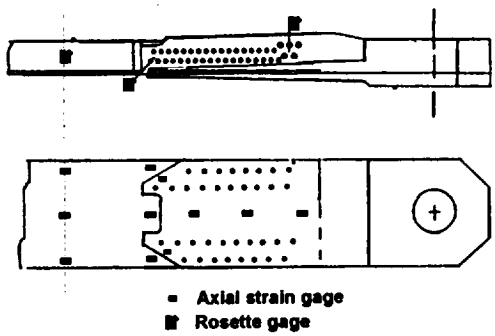

Figure 13. - Location of strain gages on tension test specimen.

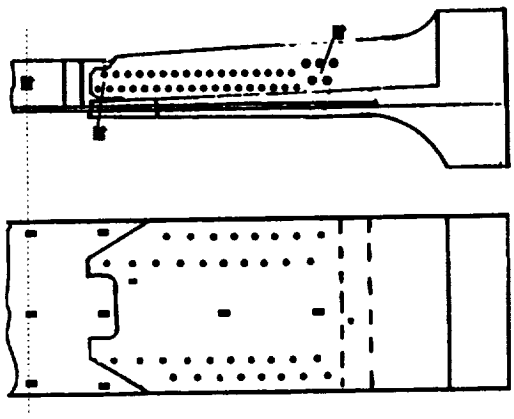

Figure 14. - Location of strain gages on compression test specimen.

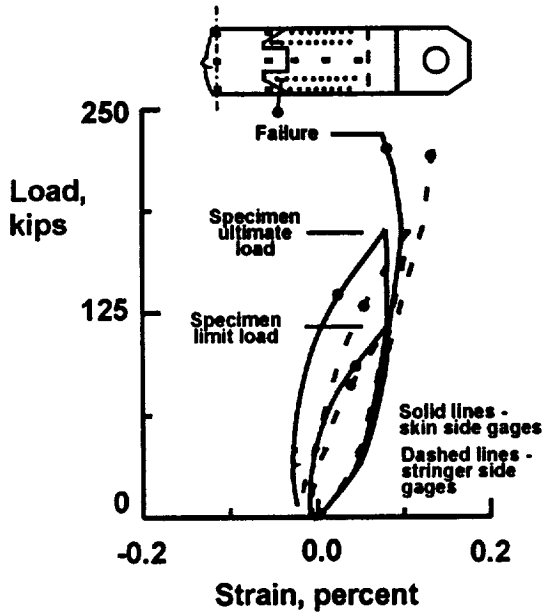

Figure 15. - Strain gage results at location between bolts 209 and 210 (see figure 8).

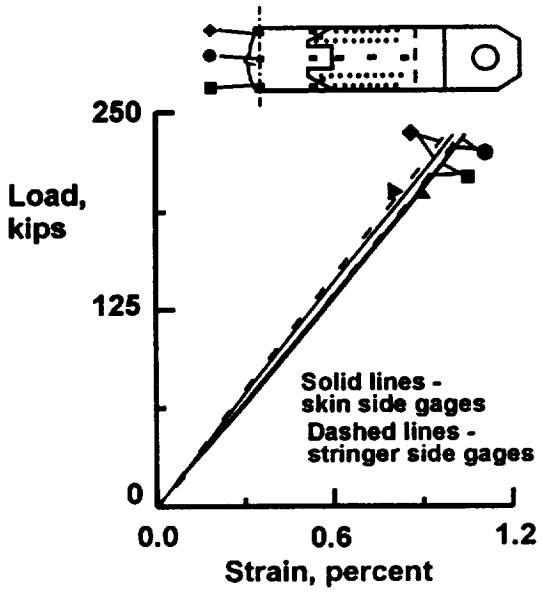

a.) Specimen T-1

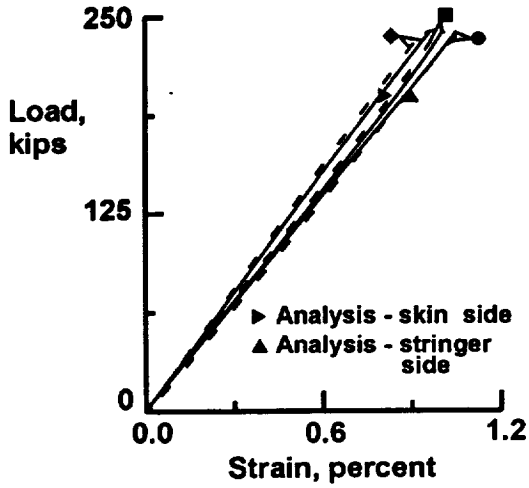

b.) Specimen T-2

Figure 16. - Strain gage results at centerline of specimen.

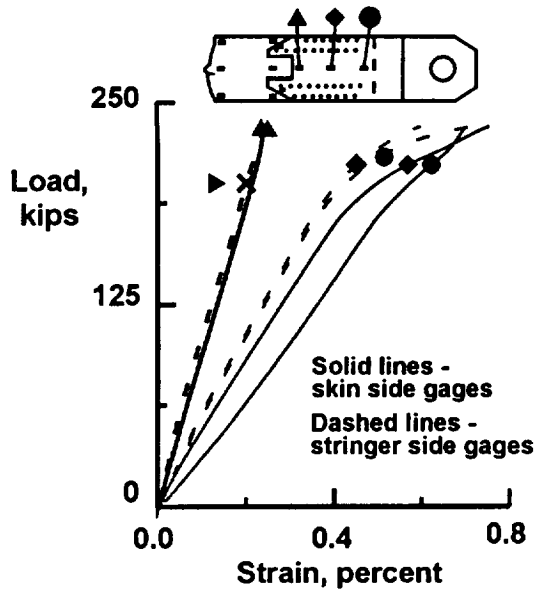

a.) Specimen T-1

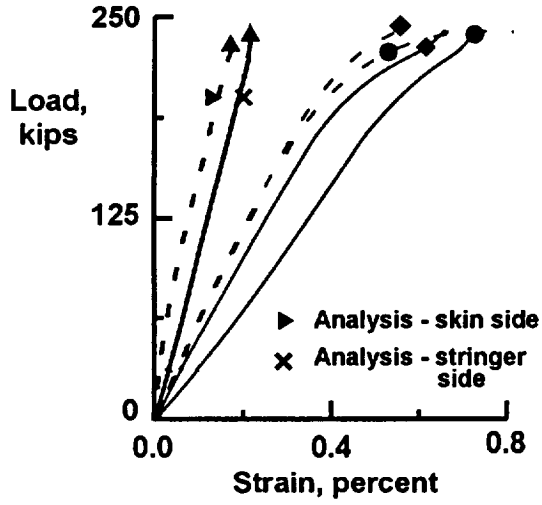

b.) Specimen T-2

Figure 17. - Strain gage results in aluminum fitting of tension specimen.

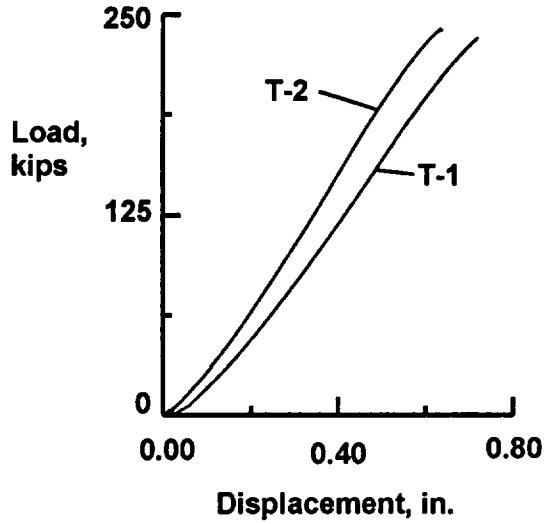

Figure 18. - Elongation of tension specimens between loading pins.

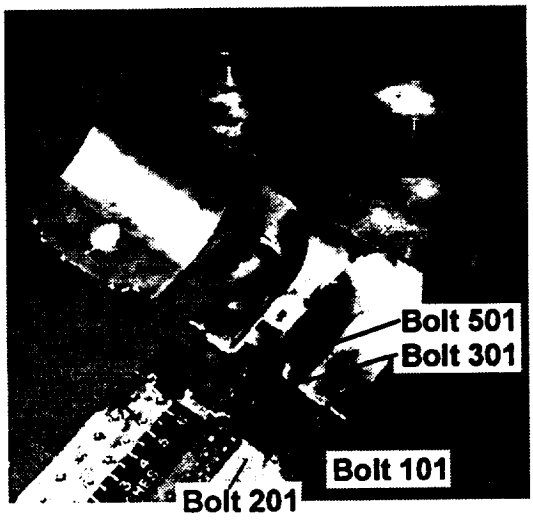

a.) Specimen T-1

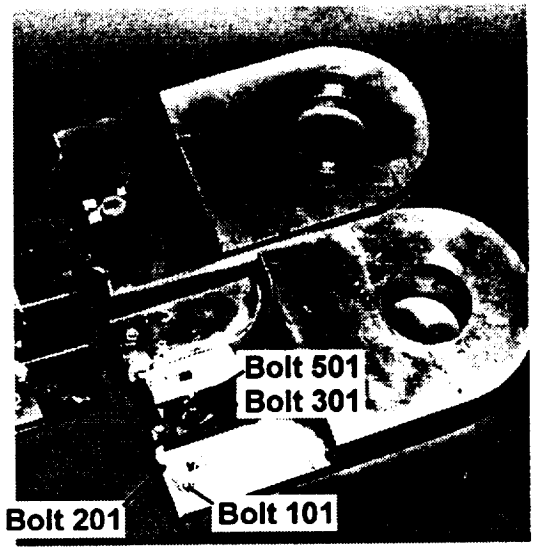

b.) Specimen T-2

Figure 19. - Failed tension test specimens.

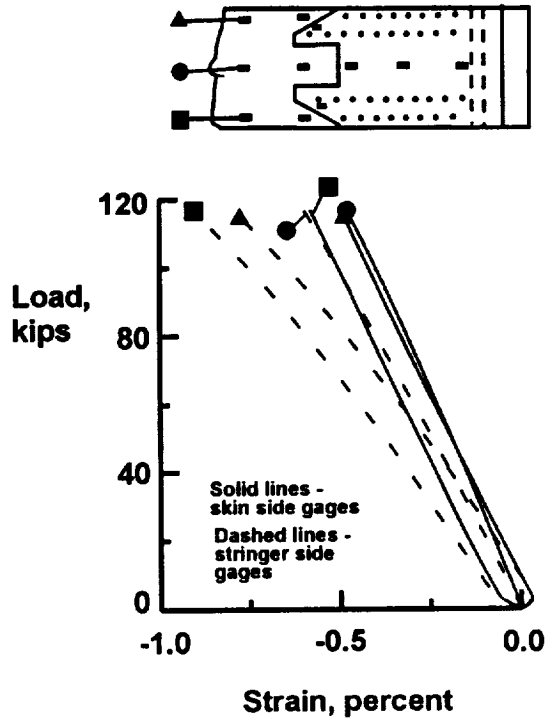

Figure 20. - Strain gage results at centerline of specimen C-1 when loaded to specimen limit load.

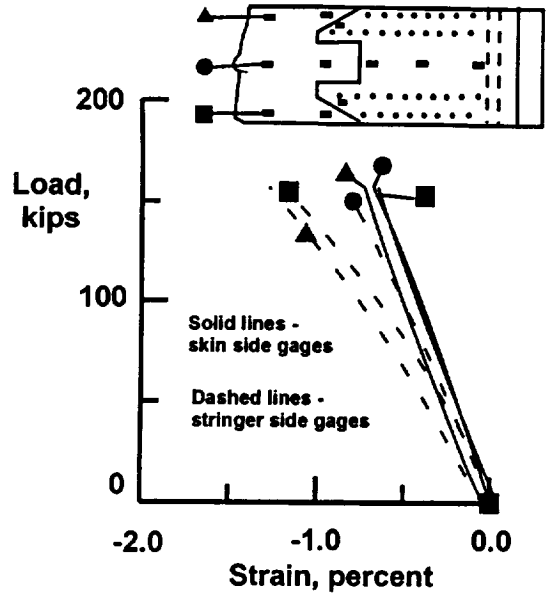

a.) Specimen C-1

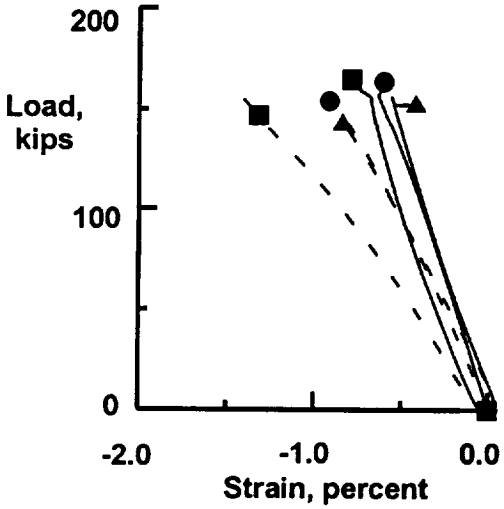

b.) Specimen C-2

Figure 21. - Strain gage results at centerline of compression specimens.

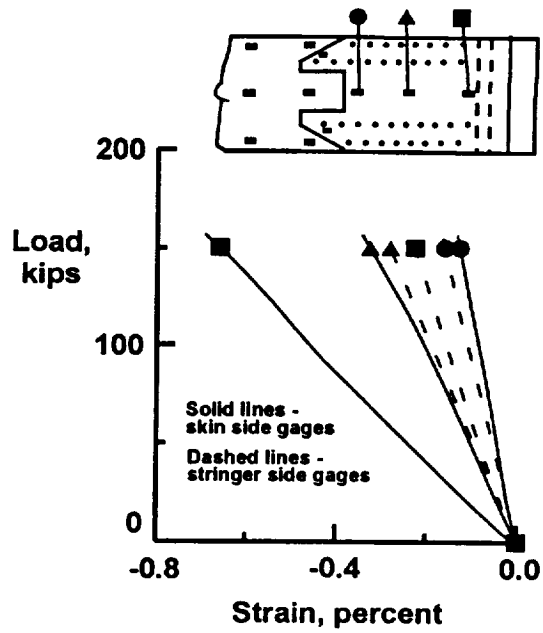

a.) Specimen C-1

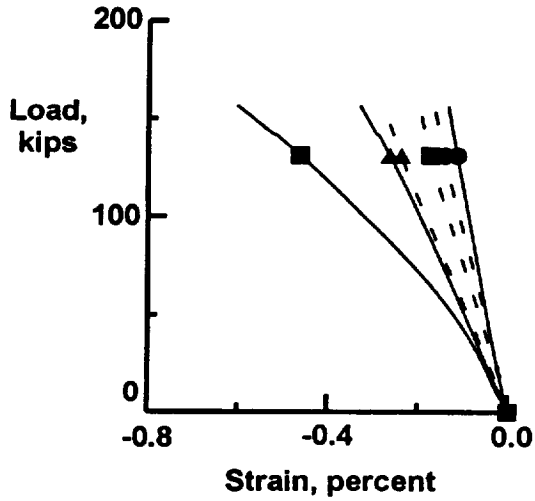

b.) Specimen C-2

Figure 22. - Out-of-plane deflection at centerline of compression specimens.

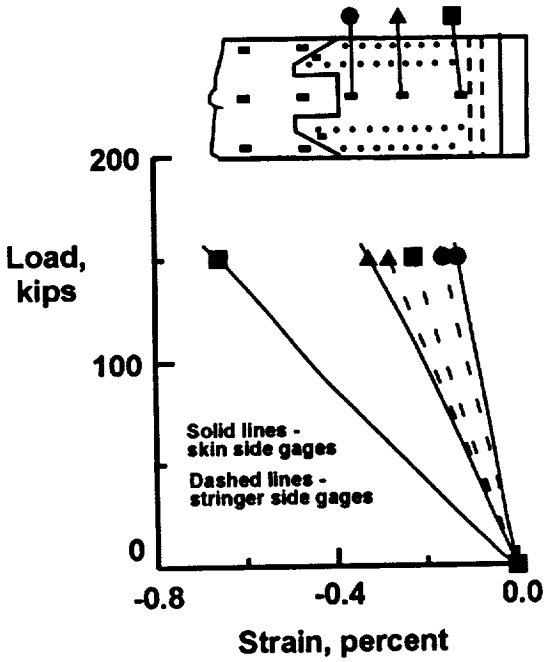

a.) Specimen C-1

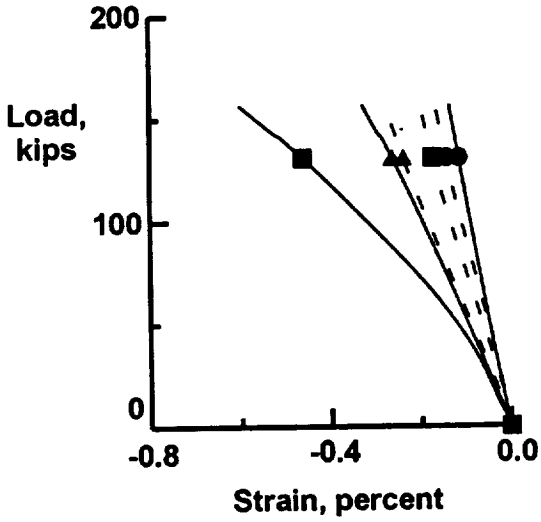

b.) Specimen C-2

Figure 23. - Strain gage results on centerline of aluminum fitting.

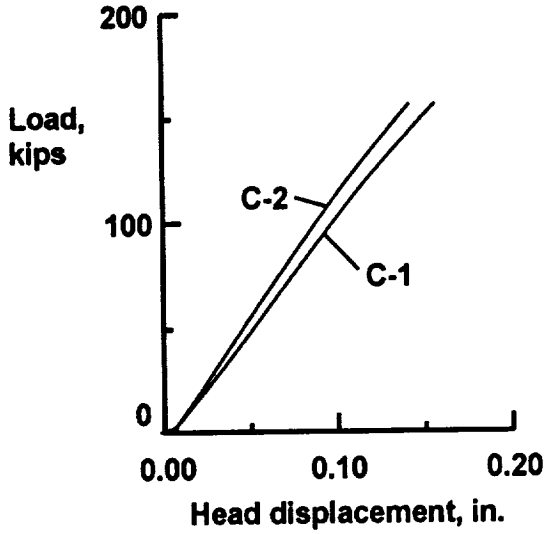

Figure 24. - Shortening of the compression specimens.

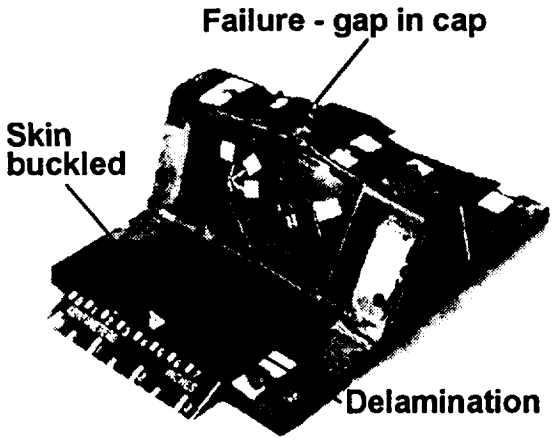

a.) Specimen C-1

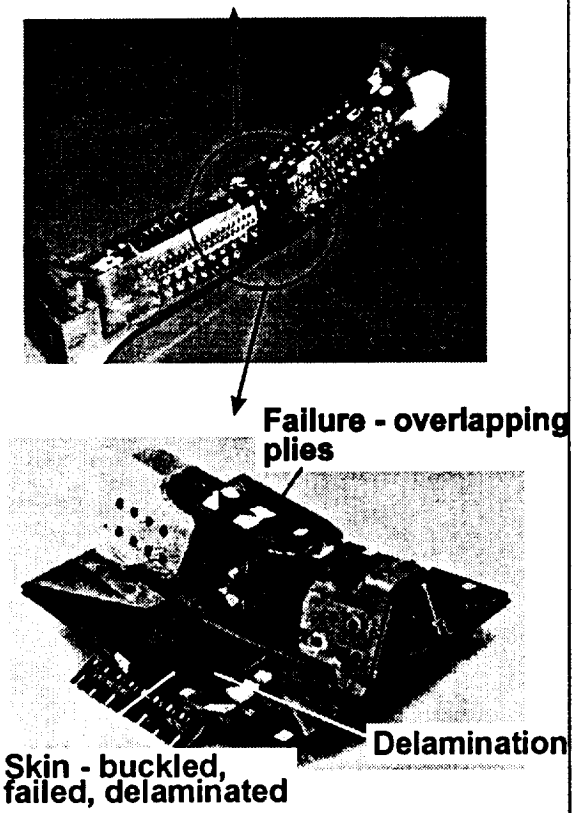

b.) Specimen C-2

Figure 25. - Failed compression specimens.

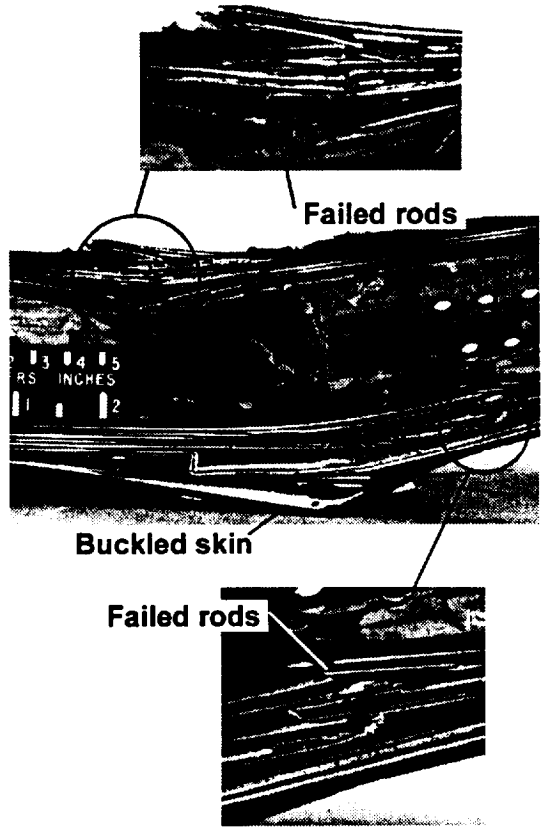

Figure 26. - Sectional view of failed specimen C-2.